Available online at www.sciencedirect.com
SCIENCE DIRECT®
Journal of Power Sources 125 (2004) 228–235
JOURNAL OF POWER SOURCES
www.elsevier.com/locate/jpowsour

An observation of peak split in high temperature CV studies on Li-stoichiometric spinel $LiMn_2O_4$ electrode

Shuhua Ma*, Hideyuki Noguchi, Masaki Yoshio

Department of Applied Chemistry, Saga University, Saga 840-0852, Japan

Received 19 May 2003; received in revised form 6 August 2003; accepted 13 August 2003

Abstract

The high temperature cyclic voltammetric performances of various Li–Mn–O spinel materials were investigated. A split of the second reduction peak at $x > 0.5$, in $Li_xMn_2O_4$, during insertion was found at temperatures higher than 70 °C, which is a characteristic of Li-stoichiometric Li–Mn–O spinel. The disproportionation dissolution of stoichiometric spinel intensified by the elevated temperature in slightly acidic electrolyte is considered responsible for the occurrence of the phenomenon. The electrochemical characteristics and dependence of the peak split on material natures, preparation temperatures, scan rates, electrolyte solvents and salts species are also presented.

Keywords: Lithium ion cell; Cathode; Li–Mn–O spinel; High temperature performance; Cyclic voltammetry; Peak split

1. Introduction

Spinel structure Li–Mn–O compounds are the most promising lithium ion insertion electrode materials for rechargeable lithium batteries because of a number of advantages over their alternatives, e.g., a lower cost compared with $LiCoO_2$ or $LiNiO_2$, a high cell voltage, and a high environmental tolerance, etc. A problem, which prevented these compounds from being commercialized, is their capacity fading during extended cycling at room temperature and elevated temperatures [1,2]. In view of the commonness of extended cycling, and both storage and cycling at elevated temperature for the consumer applications of lithium ion battery, a lot of research works have been conducted for the ascertainment of fading mechanism and the improvement of rechargeability. The capacity loss, thus far, is mainly attributed to the following several possible factors: the oxidative decomposition of electrolyte on positive electrode catalytically or at high voltage [3], the instability of spinel in electrolyte solution at elevated temperatures according to the disproportionation reaction, $2Mn^{3+} \rightarrow Mn^{4+} + Mn^{2+}$ [4], the onset of the Jahn–Teller effect in deeply discharged state [5,6] and the transformation of unstable two-phase to more stable one-phase structure via the dissolution with the loss of MnO and/or Mn_2O_3 [7,8].

In order to overcome the capacity fading at elevated temperature, the comprehensive investigations on the high temperature electrochemical performance of the spinel cathode are necessary. In this paper, we report on a new phenomenon found in the cyclic voltammetric (CV) study of Li-stoichiometric spinel electrode at temperatures higher than 70 °C, in which the second reduction peak at the latter half intercalation stage, $x > 0.5$ in $Li_xMn_2O_{4.014}$, has split, whereas this phenomenon is not observed for nonstoichiometric spinel. The split is presumably considered relating to the disproportionation dissolution of stoichiometric spinel intensified by the elevated temperature in slightly acidic electrolyte, which brought on the degradation of Li-stoichiometric spinel phase into some oxygen-deficient spinels and soluble MnO.

2. Experimental

2.1. Sample, preparation and characterization

Nine samples were examined in this study. Three of them, NS (Li-nonstoichiometric spinel), SS (Li-stoichiometric spinel) and $Li_{1.04}Cr_{0.1}Mn_{1.9}O_4$ obtained from Tosoh Co. Ltd., and other Li-stoichiometric spinel samples, $LiMn_2O_{4\pm z}$,

* Corresponding author. Present address: Research & Development Group, PEM Project, Asahi KASEI Corporation, 1-3-1, Yakoh, Kawasaki-Ku, Kawasaki-City 210-0863, Kanagawa, Japan. Tel.: +81-44-271-3260; fax: +81-44-271-2355.
E-mail address: ma.sb@om.asahi-kasei.co.jp (S. Ma).

0378-7753/$ – see front matter © 2003 Elsevier B.V. All rights reserved.
doi:10.1016/j.jpowsour.2003.08.010

and Cr-doped Li-stoichiometric spinel, $LiCr_{0.1}Mn_{1.9}O_4$, were prepared by the melt-impregnation method developed in this laboratory [9,10]. The stoichiometric mixture, molar ratio Li/Mn = 0.5, of γ-MnOOH (Tosoh Co. Ltd.) and $LiOH{\cdot}H_2O$ (Katayama Chemical) was ground well in a mortar. After mixing, the mixture was preheated at 450 °C for 12 h in air. During this process, LiOH was melted and impregnated into the pore of manganese oxide, which were formed by the thermal decomposition of the γ-MnOOH. The mixture was cooled, ground, and reheated at different temperatures of 650–900 °C, and then held for 24 h in air following a slow cooling of 20 h to room temperature (RT). The structures of all the samples were determined by X-ray diffraction (XRD) analysis. Inductively coupled plasma atomic emission spectrometry (ICP; SPS7800 plasma spectrometer from Seiko Instruments Inc.) and chemical analysis were used to determine the chemical compositions.

2.2. Electrochemical measurements

A three-electrode glass cell, consisting of a working electrode, a reference electrode (lithium foil pressed onto a stainless steel gauze) and a counter electrode (made the same way as the reference electrode), was used for cyclic voltammetric measurements. The working electrode is a pellet, consisting of 8 mg of tested material and 4 mg of conducting binder TAB-2 (Teflonized Acetylene Black), compacted onto a stainless steel gauze disk. The CV measurements were performed with an Arbin Instruments model MSTAT4 battery test system at 0.2 mV s^{-1} scan rate between the voltage limits of 3–4.5 V, except where otherwise specified.

3. Results

3.1. Structural and chemical characterization of samples

Fig. 1 shows the powder X-ray diffraction patterns of the nine samples used in this study. The patterns could be indexed to $Fd\bar{3}m$ space group with cubic symmetry. Lattice constants, surface areas and chemical compositions of the various samples are given in Table 1. SS and the samples prepared at 650, 700 and 750 °C are typical oxygen-rich Li–Mn–O spinel, whereas the samples prepared at 850 and 900 °C are oxygen-deficient Li–Mn–O spinel. With an increase of the preparation temperature, the lattice constant increases, and the samples loose more oxygen. The samples prepared at 850 and 900 °C are oxygen-deficient ones, with an increased extent along with the increase of the heating temperatures. NS is a lithium-rich Li–Mn–O spinel with a smaller cell constant, due to the increased Mn^{4+} content and the substitution of Li with smaller radius for Mn in 16d sites. Similarly, the Cr-doped Li-stoichiometric spinel, $LiCr_{0.1}Mn_{1.9}O_4$, also showed a larger lattice parameter compared to Li-nonstoichiometric Cr-doping spinel, $Li_{1.04}Cr_{0.1}Mn_{1.9}O_4$.

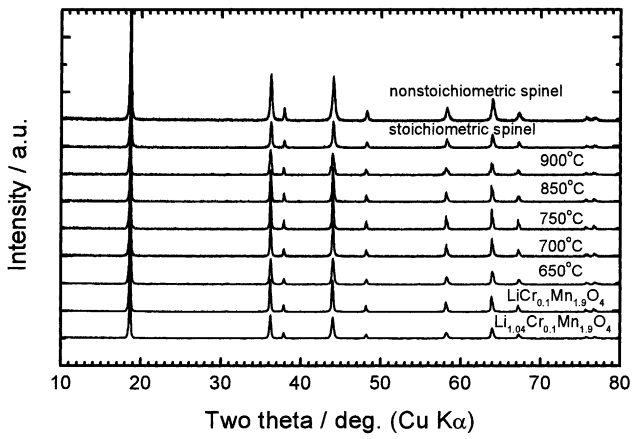

Fig. 1. Powder X-ray diffraction patterns of various Li–Mn–O and Cr-doped Li–Mn–O spinel samples.

The surface area showed a large difference, which extremely depends on the preparation temperatures for the Li-stoichiometric spinels. For example, it decreased rapidly from 7.38 $m^2 g^{-1}$ at 650 °C to 0.84 $m^2 g^{-1}$ at 900 °C as an increase in heating temperature. Meanwhile, Li-stoichiometric and Li-nonstoichiometric Cr-doped spinels gave contact surface areas of ca. 2.00 $m^2 g^{-1}$.

Table 1
Chemical composition, lattice parameter and surface area for the samples used

Sample	Composition[a]	Cell constant (a_0, Å)	Surface area ($m^2 g^{-1}$)
NS (nonstoichiometric spinel, Tosoh Co. Ltd.)	$Li_{1.063}Mn_2O_4$	8.2320	1.35
SS (stoichiometric spinel, Tosoh Co. Ltd.)	$LiMn_2O_{4.014}$	8.2346	5.26
650 °C	$LiMn_2O_{4.069}$	8.2355	7.38
700 °C	$LiMn_2O_{4.063}$	8.2384	5.30
750 °C	$LiMn_2O_{4.040}$	8.2417	3.18
850 °C	$LiMn_2O_{3.988}$	8.2435	1.03
900 °C	$LiMn_2O_{3.986}$	8.2472	0.84
$LiCr_{0.1}Mn_{1.9}O_4$	–	8.2435	2.00
$Li_{1.04}Cr_{0.1}Mn_{1.9}O_4$ (Tosoh Co. Ltd.)	–	8.2370	2.32

[a] The composition data were determined by chemical titration and ICP measurements.

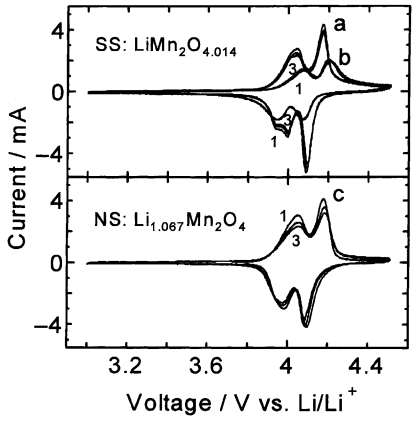

Fig. 2. Cyclic voltammograms of SS and NS electrodes in electrolyte of 1 M $LiPF_6$ EC/DMC 1:2 (v/v) with numbers referring to cycles: (a and c) the first three cycles at 85 °C; (b) the first three cycles at room temperature after being moved out from hot box and cooled. Scan rate: 0.2 mV s^{-1}; scan range: 3–4.5 V vs. Li/Li^+.

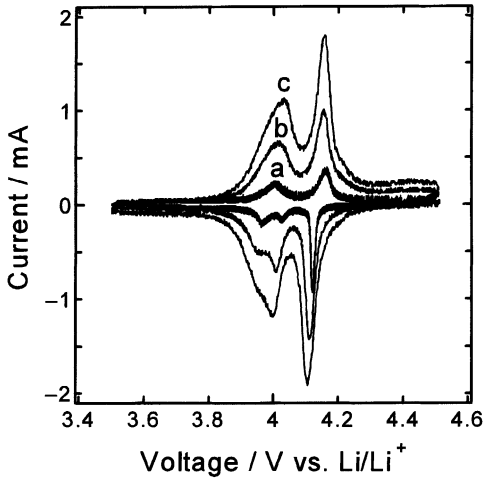

Fig. 3. Cyclic voltammograms of SS electrode in the electrolyte of 1 M $LiPF_6$ EC/DMC 1:2 (v/v) at 85 °C with different scan rates: (a) 0.01 mV s^{-1}; (b) 0.05 mV s^{-1}; (c) 0.1 mV s^{-1}.

3.2. Cyclic voltammetric performance at high temperature

Fig. 2 shows the first three CV cycles of Li/1M $LiPF_6$ EC/DMC 1:2 (v/v)/SS and NS cells at 85 °C. A clear split of the second reduction peak at the latter half intercalation stage, $x > 0.5$ in $Li_xMn_2O_{4.014}$, can be observed from the high temperature cyclic voltammogram of SS. After three scans, the cell was moved out from the hot box, cooled to room temperature, and re-scanned in the same conditions. No peak split was observed except the separation between anodic and cathodic potentials, $E_{pa} - E_{pc}$, became large and the peak currents, i_{pa} and i_{pc}, became small. For nonstoichiometric NS electrode, however, no split was found even at 85 °C. To our knowledge, there have been no reports on the split of the second reduction peak at high temperature so far. From the above results, the split is a characteristic feature of Li-stoichiometric spinel at high temperature, and at room temperature and for Li-nonstoichiometric spinel no peak split was found.

In order to clarify what dependence and properties the split has, and what is the source of the split, we carried out some experimental studies on it.

3.3. Effect of scan rates on split

Fig. 3 displays the effect of scan rates on the split. As shown in Fig. 3 for SS electrode, at a lower scan rate, 0.01 mV s^{-1}, a well-defined split, with a higher low-voltage peak, was found. With an increase of scan rate, the peak at low voltage increased, but became lower than the peak at high voltage, and finally the split disappeared at more than 0.1 mV s^{-1} of scan rate. Relationship between peak currents, I_p, of various redox peaks in Fig. 3 and the square root of scan rate is shown in Fig. 4. The peak currents of all the five peaks increased linearly as an increase in $\nu^{1/2}$. The above results suggested that the split peak also stemmed from the insertion reaction of Li^+ in solid substrate just like the normal intercalation of Li^+ in spinel as a process controlled by solid state diffusion of Li^+ ions. Moreover, in a short time domain the rate of the split-peak-relating reaction is inferior to that of the insertion of Li^+ in normal spinel. The result illuminated that the split maybe originates from a dissolution-relating process, which was characterized by a limiting reactant substrate quantity.

3.4. Effect of operating temperature on split

Fig. 5 shows cyclic voltammetric performances of NS and SS electrodes at different temperatures. It can be found that the split of the second reduction peak occurred only at the experimental temperatures of more than

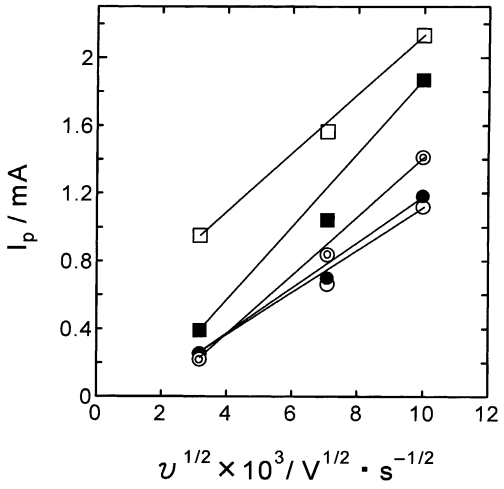

Fig. 4. Relationship between peak current, I_p, of various redox peaks in Fig. 3 and square root of scan rate, $\nu^{1/2}$. Oxidation branch: solid circle, 4.00 V; solid square, 4.16 V. Reduction branch: empty circle, 3.97 V; double circle, 4.03 V; empty square, 4.10 V.

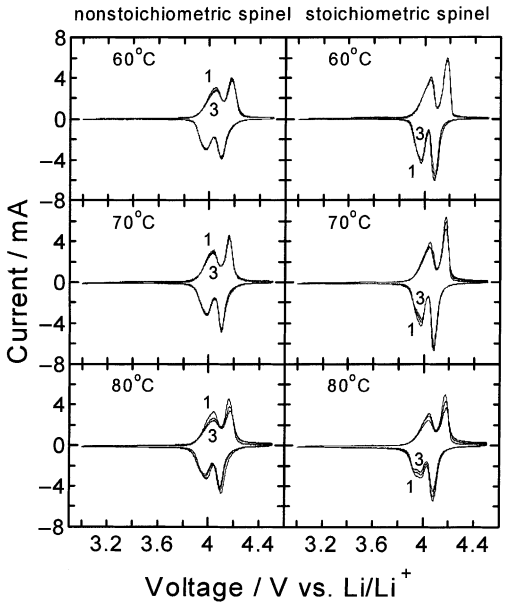

Fig. 5. First three cycles of cyclic voltammograms of nonstoichiometric (NS) and stoichiometric (SS) spinel electrodes in the electrolyte of 1 M $LiPF_6$ EC/DMC 1:2 (v/v) at different experimental temperatures with the numbers referring to cycles. Scan rate: 0.2 mV s^{-1}; scan range: 3–4.5 V vs. Li/Li^+.

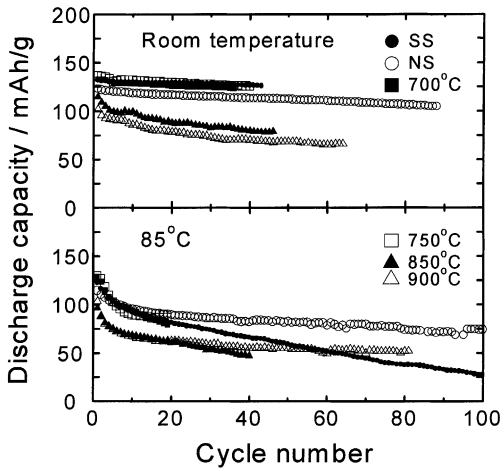

Fig. 6. Variation of specific discharge capacity with the number of cycles for various Li–Mn–O spinel samples at room temperature and 85 °C with the symbol shapes referring to sample name and preparation temperature. Galvanostatic current density: 0.4 mA cm^{-2}; cycling range: 3.0–4.5 V.

70 °C for Li-stoichiometric sample; meanwhile, no split peak was found at any other lower temperatures and for Li-nonstoichiometric spinel material electrode. With an increase of operation temperature, the peak at low voltage increased relative to normal reduction peak at about 4.03 V. It indicated that the split-peak-producing reaction was intensified by temperature. A distinguishable split can be detected only beyond 70 °C. Charge/discharge cycling tests (Fig. 6 and Table 2) evidenced that the Li-nonstoichiometric spinel gave a good cycleability with 25.2% of fading rate for 35th cycle at 85 °C, whereas the fading rate for stoichiometric spinel is up to 43.3%. The results indicated that the peak split is bound up with the deterioration of the cell especially at elevated temperatures more than 70 °C.

3.5. Cyclic voltammetric responses of spinels prepared at different temperatures

The cyclic voltammetric performances of spinel samples prepared at various temperatures, with different contents of oxygen and surface areas, are given in Figs. 7 and 8. As shown in Fig. 7, oxygen-rich Li-stoichiometric spinel phase prepared at 650 °C showed the split phenomenon. With the increase of the cycle number, the split peak has relatively gone up compared with Li^+ normal insertion peak in spinel substrate at about 4.03 V. At the third cycle, the new split peak has even gone beyond the first reduction peak, $x < 0.5$ in $Li_xMn_2O_{4.069}$. The result suggested that the original spinel phase had been heavily destroyed and substantially transformed to the new phase that caused the split. From Fig. 8, an obvious split was found also for spinel samples prepared at 700, 750 °C (oxygen-rich spinel), and 850, 900 °C (oxygen-deficient spinel). Moreover, the split peak becomes smaller than the normal reduction peak at about

Table 2
Discharge capacity and fade rate of some samples used at a certain specific cycle in room temperature and 85 °C

Sample	First discharge (C_1, mAh g^{-1})	16th discharge (C_{16}, mAh g^{-1})	Fade rate (%, $(C_1 - C_{16})/C_1$)	35th discharge (C_{35}, mAh g^{-1})	Fade rate (%, $(C_1 - C_{35})/C_1$)	Temperature (°C)
SS	131.1	128.9	1.67	127.1	3.05	RT
NS	122.6	117.1	4.53	113.8	7.20	RT
700 °C	132.7	126.9	4.41	123.4	7.05	RT
750 °C	136.4	130.2	4.54	126.0	7.63	RT
850 °C	114.5	91.88	19.7	83.17	27.3	RT
900 °C	101.3	79.92	21.1	70.17	30.7	RT
SS	122.6	85.06	30.6	69.49	43.3	85
NS	114.3	91.45	20.0	85.56	25.2	85
700 °C	128.6	84.00	34.7	49.48	61.5	85
750 °C	126.8	81.67	35.6	–	–	85
850 °C	96.40	64.44	33.2	50.65	47.5	85
900 °C	103.4	62.62	39.4	56.21	45.6	85

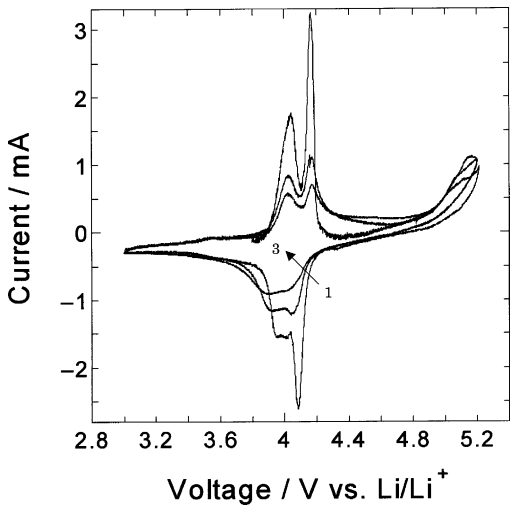

Fig. 7. First three cycles of cyclic voltammograms of oxygen-rich Li-stoichiometric spinel prepared at 650 °C in the electrolyte of 1M $LiPF_6$ EC/DMC 1:2 (v/v) at 85 °C with the numbers referring to cycles. Scan rate: 0.2 mV s^{-1}; scan range: 3–5.2 V vs. Li/Li^+.

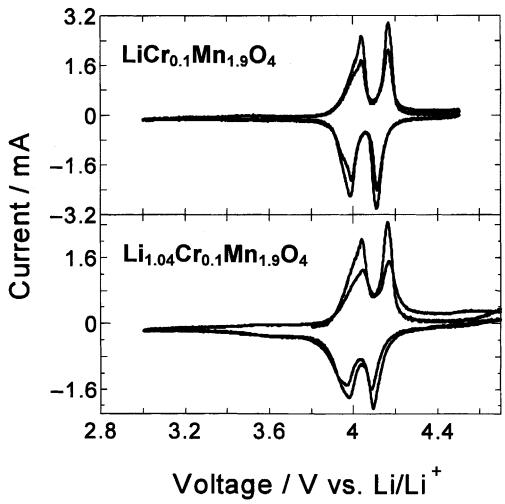

Fig. 9. First two cycles of cyclic voltammograms of Cr-doped Li-stoichiometric and Li-nonstoichiometric spinels in the electrolyte of 1 M $LiPF_6$ EC/DMC 1:2 (v/v) at 85 °C. Scan rate: 0.1 mV s^{-1}; scan range: 3–4.5 or 5.2 V vs. Li/Li^+.

4.03 V. As the surface area and oxygen content decreased, i.e., the preparation temperature increased, the split peak at low voltage decreased relative to normal second insertion peak of spinel. The results demonstrated that the split is enhanced by the higher surface area, which indicated its nature from a dissolution process. It should be noted that the split also could be found even for the sample treated at 900 °C with a smaller surface area of 0.84 m^2 g^{-1}. Here, no heavy dissolution can be expected in view of the small surface area. The result suggests that oxygen-deficiency itself played an important role in the peak split. It has been shown in Fig. 6 that both the Li-nonstoichiometric spinel, NS, and Li-stoichiometric oxygen-deficient spinel prepared at 900 °C exhibited improved stability in electrolyte at high temperature in comparison with Li-stoichiometric Li–Mn–O spinels, SS, although the Li-stoichiometric oxygen-deficient spinel prepared at 900 °C gave a smaller capacity.

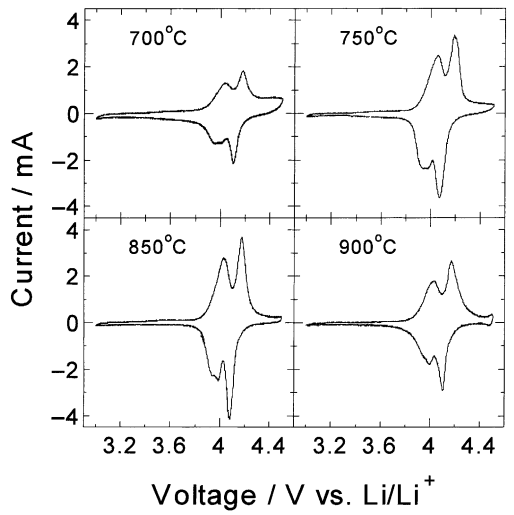

Fig. 8. Cyclic voltammograms of various Li-stoichiometric Li–Mn–O spinel samples prepared at 700, 750, 850 and 900 °C in the electrolyte of 1 M $LiPF_6$ EC/DMC 1:2 (v/v) at 85 °C. Scan rate: 0.2 mV s^{-1}; scan range: 3–4.5 V vs. Li/Li^+.

3.6. CV responses of Li-stoichiometric and Li-nonstoichiometric Cr-doped Li–Mn–O spinels

CV responses of Li-stoichiometric and Li-nonstoichiometric Cr-doped Li–Mn–O spinels at elevated temperature were also investigated. From Fig. 9, the split phenomenon occurred for both the Li-stoichiometric and Li-nonstoichiometric spinels, $LiCr_{0.1}Mn_{1.9}O_4$ and $Li_{1.04}Cr_{0.1}Mn_{1.9}O_4$; moreover, distinct oxidation peak splits can be detected. But the splits have been suppressed by the doping of Cr to Mn in 16d sites. A small peak split for $LiCr_{0.1}Mn_{1.9}O_4$ was obtained, compared with the case of SS (Fig. 2). Furthermore, from the indistinct peak split for Li-nonstoichiometric $Li_{1.04}Cr_{0.1}Mn_{1.9}O_4$, the suppression effect of Li nonstoichiometry on peak splitting was affirmed. The result demonstrated Li stoichiometry of spinel is related with the peak split. Due to the doping of Li, Cr to Mn in octahedral 16d sites, the splits were considerably attenuated in comparison with the normal Li insertion peak. It has been reported that the doping of Li and Cr to Mn improved stability of spinel structure and its cell cycleability [11,12].

3.7. Effects of electrolyte solvents and salts on split

Various salts and solvents were used to understand the effects of electrolyte components on peak split. Fig. 10 showed the influence of electrolytes on high temperature CV behavior of stoichiometric spinel electrode, SS. Clear splits of the second reduction peak were observed for all the three electrolytes. No special effect from the electrolyte components

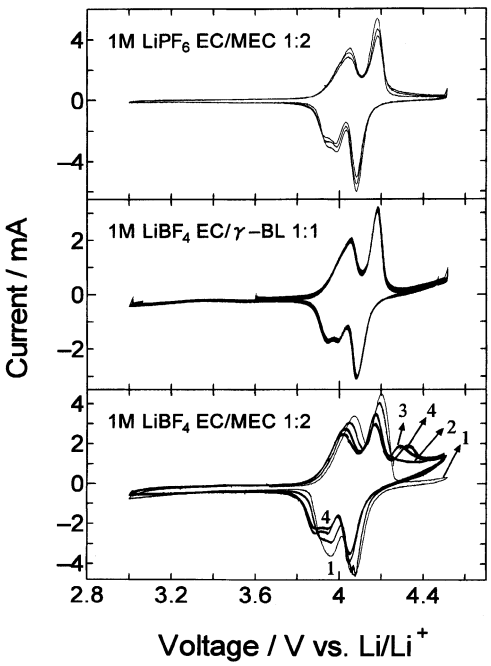

Fig. 10. Cyclic voltammograms of SS electrode in electrolytes of 1 M $LiPF_6$ EC/MEC 1:2 (v/v), 1 M $LiBF_4$ EC/γ-butyrolactone 1:1 (v/v) and 1 M $LiBF_4$ EC/MEC 1:2 (v/v) at 85 °C. Scan rate: 0.1 mV s^{-1}; scan range: 3–4.5 V vs. Li/Li^+.

could be found for the reduction peak split. Further, in 1 M $LiBF_4$ EC/MEC 1:2 (v/v) electrolyte, a new oxidation peak near 4.35 V arose at third cycles along with the split of the second reduction peak at the same time, which exhibits the split's relevance to dissolution process in electrolyte. The concurrence of the split peak and the new oxidation peak near 4.35 V confirmed their pairing, although the oxidation peak has been held up to 4.35 V.

4. Discussion

All above data showed that the split phenomenon is relating to the stability of the Li–Mn–O spinel, i.e., Li stoichiometry and the doping of foreign metal ions, e.g., Li^+ and Cr^{3+}, in Li–Mn–O spinel structure. Meanwhile, the surface area played an important role, which would be expected to take effect through a dissolution process. Furthermore, the oxygen-deficient spinel was considered as a direct source causing the split of the reduction peak.

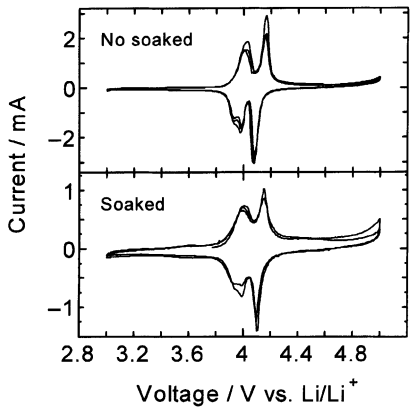

Fig. 11. Cyclic voltammograms at 80 °C of $LiMn_2O_{4.014}$ before and after soaking for 24 h in 80 °C in electrolyte of 1 M $LiPF_6$ EC/DMC 1:2 (v/v). Scan rate: 0.1 mV s^{-1}; scan range: 3–5.0 V vs. Li/Li^+.

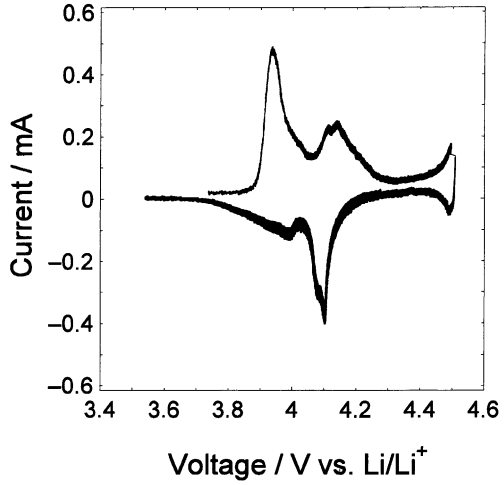

Fig. 12. First cycle of cyclic voltammogram of $LiMn_2O_{3.912}$ prepared at 950 °C following a slow cooling of 10 h to room temperature in 1 M $LiPF_6$ EC/DMC 1:2 (v/v) at 85 °C. Scan rate: 0.02 mV s^{-1}; voltage range: 3.4–4.5 V.

4.1. On dissolution of Li–Mn–O spinel in electrolyte

In view of stability of Li-stoichiometric and Li-nonstoichiometric spinels in electrolyte, the dissolution reaction could be considered as an origin of the peak split. The soaking experiment of various Li–Mn–O spinel samples in 1 M

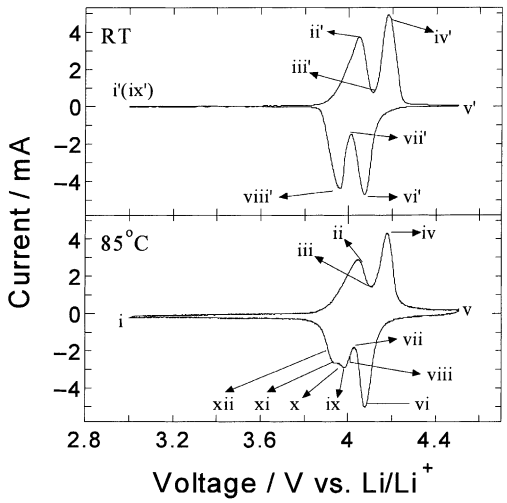

Fig. 13. Cyclic voltammograms of $LiMn_2O_{4.014}$ electrode in the electrolyte of 1 M $LiPF_6$ EC/DMC 1:2 (v/v) at room temperature and 85 °C. Scan rate: 0.2 mV s^{-1}; scan range: 3–4.5 V vs. Li/Li^+. The Roman numbers refer to the specific insertion/extraction states indicated in X-ray diffraction patterns of Figs. 14 and 15.

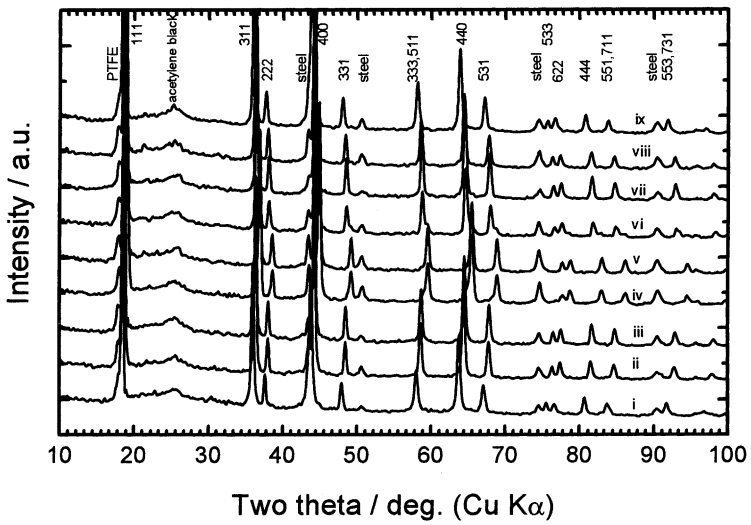

Fig. 14. X-ray diffraction patterns at different charge/discharge states of stoichiometric $LiMn_2O_{4.014}$ spinel electrode at room temperature. The Roman numbers refer to the specific insertion/extraction states indicated in Fig. 13.

$LiPF_6$ EC/DMC 1:2 (v/v) electrolyte showed that dissolution of Li–Mn–O spinel sample is related with the surface area and is suppressed by the substitutions of foreign metal ions into Mn in octahedral sites. When soaked the sample powders in 1 M $LiPF_6$ EC/DMC 1:2 (v/v) electrolyte at 85 °C, the characteristic red purple color of MnO, a soluble dissolution product, was found after 2 h for the sample prepared at 650 °C, whereas, a weak color after soaking 10 h for that prepared at 900 °C. Meanwhile, the electrolyte became red purple after 4 h for SS and 15 h for NS.

Fig. 11 showed the cyclic voltammograms at 80 °C of SS before and after soaking for 24 h in 80 °C in electrolyte of 1 M $LiPF_6$ EC/DMC 1:2 (v/v). It can be found that both the oxidation and reduction parts at about 4.5 V, which is related to oxygen and lithium deficiencies in spinel structure, were raised and the normal two pairs of redox peaks became poorly separated after the soaking. The results suggest that the sample has become oxygen and lithium deficient after the soaking.

4.2. On origin of the split

In order to further clarify the real origin of the peak split, we prepared the Li–Mn–O sample at 1000 °C following a slow cooling of 10 h down to RT. A highly oxygen-deficient Li–Mn–O spinel, $LiMn_2O_{3.912}$, was obtained. The first CV curve at 85 °C is shown in Fig. 12, peak splits of both the two pairs of redox peaks can be found. The result showed that oxygen-deficient spinel in high temperature resulted in the split. Some phase separation may be responsible for

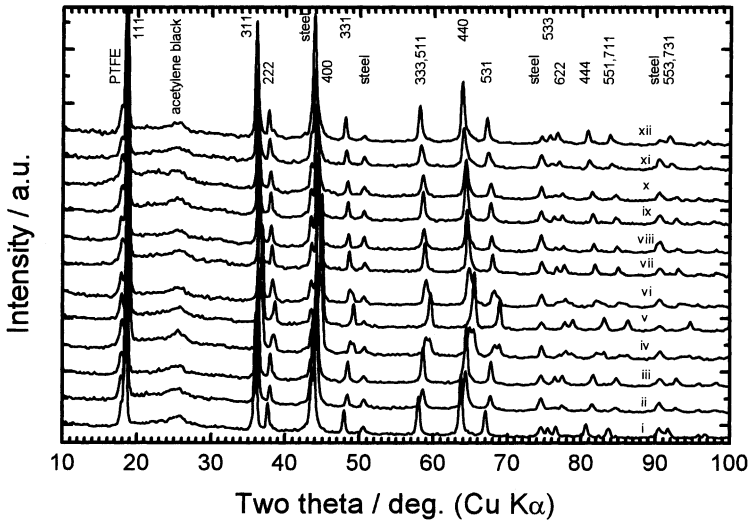

Fig. 15. X-ray diffraction patterns at different charge/discharge states of stoichiometric $LiMn_2O_{4.014}$ spinel electrode at 85 °C. The Roman numbers refer to the specific insertion/extraction states indicated in Fig. 13.

the split phenomenon [13,14]. We have carried out XRD measurements for the sample electrodes cycled in both RT and 85 °C to identify these phases. The results are shown in Figs. 13–15. Unfortunately, no discernible new phase can be detected. From the data in Fig. 2, the split is characteristic of high temperature. High temperature in situ XRD would be an effective means to isolate these new phases.

5. Conclusions

The high temperature cyclic voltammetric performances of Li–Mn–O spinel material electrodes were studied. At higher than 70 °C, for stoichiometric Li–Mn–O spinel, a split phenomenon of the second reduction peak at $x > 0.5$ in $Li_xMn_2O_4$ during insertion was found.

The wide studies on various samples with different lithium and oxygen contents not only confirmed the existence of the split, but also demonstrated its characteristics of Li-stoichiometric Li–Mn–O spinel, which is related to the instability of spinel in electrolyte.

The excess of Li and substitution of Cr to Mn and small surface area impeded the occurrence of the split. The split is presumably considered relating to the disproportionation dissolution of stoichiometric spinel intensified by the elevated temperatures in slightly acidic electrolyte due to residual water impurity.

Oxygen-deficient spinel was identified as the insoluble dissolution product, which caused the split at high temperature more than 70 °C.

Acknowledgements

The authors are grateful to the grants-in-aid for Scientific Research from the Japanese Ministry of Education for financial support of this research.

References

[1] D. Guyomard, J.M. Tarascon, J. Electrochem. Soc. 139 (1991) 937.
[2] A. Momchilov, V. Manev, A. Nassalevska, J. Power Sources 41 (1993) 305.
[3] D. Guyomard, J.M. Tarascon, J. Power Sources 54 (1995) 92.
[4] M.M. Thackeray, P.J. Johnson, L.A. De Picciotto, P.G. Bruce, J.B. Goodenough, Mater. Res. Bull. 19 (1984) 179.
[5] J.M. Tarascon, E. Wang, F.K. Shokoohi, W.R. McKinnon, S. Colson, J. Electrochem. Soc. 138 (1991) 2859.
[6] M.M. Thackeray, W.I.F. David, P.G. Bruce, J.B. Goodenough, Mater. Res. Bull. 18 (1983) 461.
[7] Y. Xia, H. Noguchi, M. Yoshio, J. Solid State Ionics 119 (1995) 216.
[8] Y. Xia, Y. Zhou, M. Yoshio, J. Electrochem. Soc. 144 (1997) 2593.
[9] M. Yoshio, S. Inoue, M. Hyakutake, G. Piao, H. Nakamura, J. Power Sources 34 (1991) 147.
[10] M. Yoshio, H. Noguchi, T. Miyashita, H. Nakamura, A. Kozawa, J. Power Sources 54 (1995) 483.
[11] L. Guohua, H. Ikuta, T. Uchida, M. Wakihara, J. Electrochem. Soc. 143 (1996) 178.
[12] A.D. Robertson, S.H. Lu, W.F. Howard Jr., J. Electrochem. Soc. 144 (1997) 3505.
[13] X.Q. Yang, X. Sun, S.J. Lee, J. McBreen, S. Mukerjee, M.L. Daroux, X.K. Xing, Electrochem. Solid State Lett. 2 (1999) 157.
[14] W. Liu, K. Kowal, G.C. Farrington, J. Electrochem. Soc. 145 (1998) 459.